JOURNAL OF AGRICULTURAL AND FOOD CHEMISTRY

Article

pubs.acs.org/JAFC

Hexahydro-β-Acids Potently Inhibit 12-*O*-Tetradecanoylphorbol 13-Acetate-Induced Skin Inflammation and Tumor Promotion in Mice

Chung-Huei Hsu,[†,○] Yuan-Soon Ho,[‡,§,∥,○] Ching-Shu Lai,[⊥] Shu-Chen Hsieh,[⊥] Li-Hua Chen,[⊥] Edwin Lin,[‡] Chi-Tang Ho,[#] and Min-Hsiung Pan*[,⊥,▽]

[†]Department of Nuclear Medicine, Taipei Medical University Hospital, Taipei 110, Taiwan

[‡]Department of Laboratory Medicine, Taipei Medical University Hospital, Taipei 110, Taiwan

[§]School of Medical Laboratory Science and Biotechnology, College of Medical Science and Technology, Taipei Medical University, Taipei 110, Taiwan

[∥]Center of Excellence for Cancer Research, Taipei Medical University, Taipei 110, Taiwan

[⊥]Institute of Food Science and Technology, National Taiwan University, Taipei 10617, Taiwan

[#]Department of Food Science, Rutgers University, New Brunswick, New Jersey 08901, United States

[▽]Department of Medical Research, China Medical University Hospital, China Medical University, Taichung 40402, Taiwan

ABSTRACT: We previously reported that hexahydro-beta-acids (HBAs), reduced derivatives of beta-acids (BA) from hop (*Humulus lupulus* L.), displayed more potent anti-inflammatory activity than BA in lipopolysaccharide-stimulated murine macrophages. In this study, we investigated the effects and underlying molecular mechanisms of hexahydro-β-acids (HBAs) on 12-*O*-tetradecanoylphorbol-13-acetate (TPA)-stimulated mouse skin inflammation and in the two-stage carcinogenesis model. Female ICR mice pretreated with HBA at 1 and 10 μg significantly reduced ear edema, epidermal hyperplasia, and infiltration of inflammatory cells caused by TPA. Molecular analysis exhibited that HBA suppressed iNOS, COX-2, and ornithine decarboxylase (ODC) protein and gene expression through interfering with mitogen-activated protein kinases (MAPKs) and phosphatidylinositiol 3-kinase (PI3K)/Akt signaling as well as the activation of transcription factor NF-κB. Furthermore, application of HBA (1 and 10 μg) prior to each TPA treatment (17.2 ± 0.9 tumors/mouse) resulted in the significant reduction of tumor multiplicity (5.1 ± 1.2, $P < 0.01$ and 2.3 ± 1.2, $P < 0.001$, respectively) in 7,12-dimethyl-benzanthracene (DMBA)-initiated mouse skin. The tumor incidence was significantly lowered to 75% ($P < 0.05$) and 58.7% ($P < 0.01$) by HBA pretreatment, respectively, and significantly reduced the tumor weight (0.34 ± 0.14 g, $P < 0.01$ and 0.09 ± 0.10 g, $P < 0.001$, respectively) as compared to DMBA/TPA-induced tumors (0.76 ± 0.04 g).

KEYWORDS: *cyclooxygenase-2 (COX-2), hexahydro-β-acids (HBA), inducible NO synthase (iNOS), inflammation, two-stage carcinogenesis*

INTRODUCTION

Chronic inflammation has been linked to various human diseases including cancer.[1,2] Cancer development is a multiple process characterized by limitless replication potential, evasion of apoptosis, self-sufficiency in growth signals, insensitivity to antigrowth signals, sustained angiogenesis, and tissue invasion and metastasis, whereas inflammation has been recognized as the seventh hallmark.[3] The pathological mechanism of inflammation involved in cancer development is very complicated including induction of malignant transformation and proliferation in initiated cells, promotion of angiogenesis, invasion, and metastasis of tumor cells that facilitates tumor growth.[4] Deregulation of inflammatory signaling cascades and overproduction of pro-inflammatory mediators contribute to tumorigenesis.[2,4] Therefore, suppression of inflammation should be a potential target for cancer chemopreventive strategy.

The mouse skin model has been extensively used to study the molecular changes implicated in multistep tumorigenesis.[5] In the two-stage skin carcinogenesis, the initiator 7,12-dimethyl-benzanthracene (DMBA) causes formation of DNA adducts and irreversible DNA damage, which leads to mutation of the oncogene in epidermal cells.[6] The potent tumor promoter 12-*O*-tetradecanoylphorbol-13-acetate (TPA) elicits skin inflammation, edema, and epidermal hyperplasia, further promoting DMBA-initiated papilloma formation.[7,8] Topical application of TPA in mouse skin up-regulates numbers of genes expression involved in inflammation and proliferation such as inducible nitric oxide synthase (iNOS), inducible-type cyclooxygenase (COX-2), and ODC.[9,10] Excessive expression of iNOS and COX-2 contributes to skin inflammation and tumorigenesis by production of nitric oxide (NO) and prostaglandin E_2 (PGE_2), while specific inhibitors are able to counteract these biological events.[10,11] TPA induces inflammatory genes expression by activation of NF-κB, through a cascade of events that activate inhibitor κB (IκB) kinases, which in turn phosphorylates IκB, degrades, and leads to NF-κB translocation

Received: August 11, 2013
Revised: October 26, 2013
Accepted: November 8, 2013
Published: November 8, 2013

to the nucleus.[9,11] Up-regulation of mitogen-activated protein kinases (MAPKs) and phosphatidylinositol 3-kinase (PI3K)/AKT signaling also involves cytokines or TPA-stimulated NF-κB transcriptional activity.[9,12] Inhibition of NF-κB by pyrrolidine dithiocarbamate is shown to decrease TPA-induced epidermal hyperplasia, leukocyte infiltration, and protein levels of iNOS, COX-2, and ODC.[10]

Numerous dietary natural compounds are shown to have anti-inflammatory properties[13] and act as effective chemopreventive agents through interfering with intracellular signaling,[14] suppressing production of pro-inflammatory mediators, and attenuation of inflammatory responses.[2,15] Hop (*Humulus lupulus* L.) is an essential ingredient for beer brewing and has been used in traditional medicine.[16] Hop-derived bitter acids and their oxidation products not only give the unique bitter taste and aroma of beer but also exert a wide range of biological effects, including antioxidation,[17] antibacteria,[18] anti-inflammation,[19] antifibrogenesis,[20] antitumor promotion,[21] antiangiogenesis,[22] induction of apoptosis,[23] and they have been considered as chemopreventive agents.[24] The amount of bitter acids in dried hops is up to 25% and mainly consists of α-acids (or humulones) and β-acids (lupulones; BA) that are prenylated phloroglucinol derivatives.[16] Both α-acids and β-acids are a mixture of homologues of different acyl side chains. β-acids containing lupulone, colupulone, and adlupulone are extremely sensitive to oxidation and spontaneously transformed into oxidized derivatives during storage.[16] Research demonstrates that hexahydro-β-acids (HBAs), the reduced derivatives of BAs, display stronger antibacterial and antiproliferative properties than BAs.[25,26] Hexahydrolupulone was found to be 6−8 times more active than lupulone on bacteriostatic *in vitro* tube assay. Moreover, hexahydrolupulone appears to be more stable to air for several months, while lupulone resinified after a few days.[27] Our previous study showed that HBA displayed a potent growth inhibitory effect on human leukemia HL-60 cells through induction of apoptosis, but BA was less effective.[28] Recently, we have also shown that HBA was more active than BA on suppression of lipopolysaccharide-induced inflammatory enzymes in RAW264.7 murine macrophages by blocking multiple upstream signaling and activation of NF-κB.[29] However, the exact molecular mechanisms underlying the *in vivo* anti-inflammatory and chemopreventive effect of HBA remain largely unresolved. In the present study, the effect of HBA on TPA-stimulated inflammatory response in mouse skin and the possible molecular mechanism were investigated. We also evaluated the antitumor promoting effect of HBA by using the classical two-stage mouse skin carcinogenesis model.

MATERIALS AND METHODS

Chemicals. The synthesis of HBA derived from BA was by way of hydrogenation according to the method by Liu et al.[26] The composition of HBA contained 57% hexahydrocolupulone (Figure 1, left peak) and 41% hexahydrolupulone and hexahydroadlupulone (Figure 1, right peak); the HPLC profile has been described previously.[26,28] TPA and DMBA were purchased from Sigma Chemical Co. (St Louis, MO). All other chemicals used were in the purest form available commercially.

Animals. Female Institute of Cancer Research mice at 5−6 weeks old were obtained from the BioLASCO Experimental Animal Center (Taiwan Co., Ltd., BioLASCO, Taipei, Taiwan). All animals were housed in a controlled atmosphere (25 ± 1 °C at 50% relative humidity) and with a 12 h light−12 h dark cycle. Animals had free access to food and water at all times. All animal experimental protocol used in this study was approved by Institutional Animal Care and Use Committee of the National Kaohsiung Marine University (IACUC, NKMU). After 1 week of acclimation, the dorsal skin of each mouse was shaved with surgical clippers before the application of tested compound. DMBA, TPA, and HBA were dissolved in 200 μL of acetone and applied topically to the shaved area of each mouse. Control animals were treated with acetone with the same volume as the vehicle in all experiments.

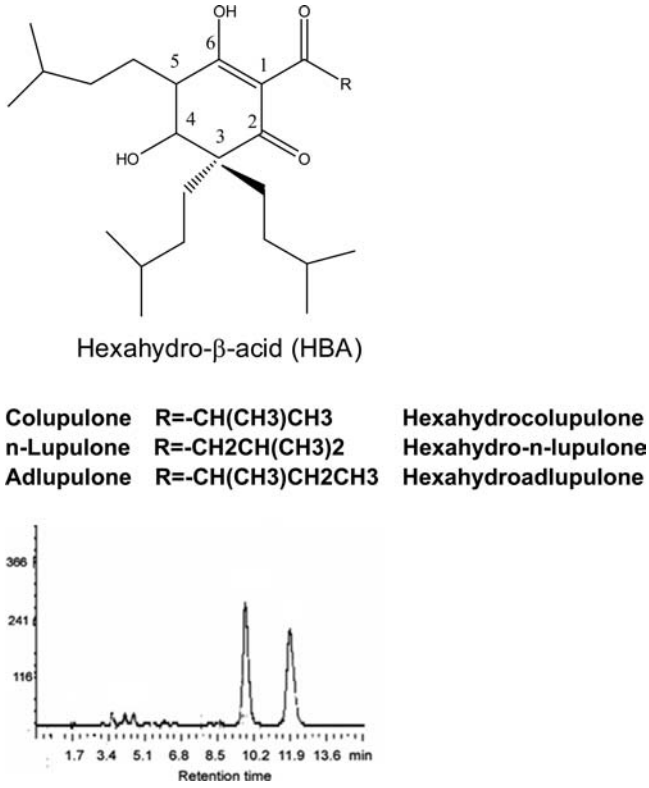

Figure 1. Chemical structures of hexahydro-β-acid (HBA).

Western Blot Analysis. Mice were topically treated with HBA on their shaved backs for 30 min before application of TPA (10 nmol). The mice were sacrificed by CO_2 asphyxiation at the indicated time. Dorsal skins of mice were excised, and the separations of epidermis and dermal fractions were performed by heat treatment (60 °C for 30 s). The epidermis was gently removed using a scalpel on ice, and the separated epidermis fractions were immediately placed in liquid nitrogen for protein extraction. The epidermis was homogenized on ice for 15 s with a Polytron tissue homogenizer and lysed in 0.2 mL of ice-cold lysis buffer [50 mM Tris−HCl, pH 7.4, 1 mM NaF, 150 mM NaCl, 1 mM ethylene glycol-bis(aminoethylether)-tetraacetic acid, 1 mM phenylmethanesulfonyl fluoride, 1% Nonidet P-40 (NP-40), and 10 μg/mL leupeptin] on ice for 30 min, followed by centrifugation at 18 000*g* for 30 min at 4 °C. The total protein in the supernatant was measured by Bio-Rad protein assay (Bio-Rad Laboratories, Munich, Germany). Equal amounts of total c protein (50 μg) were resolved by SDS−polyacrylamide minigels and transferred onto immobilon polyvinylidene difluoride membranes (Millipore, Bedford, MA). The membrane was then blocked at room temperature for 1 h with blocking solution (20 mM Tris−HCl, pH 7.4, 125 mM NaCl, 0.2% Tween 20, 1% bovine serum albumin, and 0.1% sodium azide) followed by incubation with the primary antibody, overnight, at 4 °C. The membrane was then washed with 0.2% TPBS (0.2% Tween-20/PBS) and subsequently probed with antimouse, antirabbit, or antigoat IgG antibody conjugated to horseradish peroxidase (Transduction Laboratories, Lexington, KY) and visualized using enhanced chemiluminescence (ECL, Amersham Biosciences, Buckinghamshire, U.K.). Primary antibodies of specific protein were purchased from various locations as listed: The primary antibodies used were as follows: iNOS, p50, p65, and phospho-PI3K (Tyr508) polyclonal

antibodies (Santa Cruz Biotechnology, Santa Cruz, CA); ornithine decarboxylase and COX-2 monoclonal antibodies (Transduction Laboratories, BD Biosciences, Lexington, KY); phospho-p65 (Ser536), phospho-p38 (Thr180/Tyr182), phospho-extracellular signal regulated kinase (ERK)1/2 (Thr202/Tyr204), phospho-c-Jun NH2-terminal kinase (JNK) (Thr183/Tyr185), phospho-Akt (Ser473), p38, ERK1/2, JNK, and Akt polyclonal antibodies (Cell Signaling Technology, Beverly, MA). The densities of the bands were quantitated with a computer densitometer (AlphaImagerTM 2200 System). All the membranes were stripped and reprobed for β-actin (Sigma Chemical, St Louis, MO) or lamin B (Santa Cruz Biotechnology, Santa Cruz, CA) as the loading control.

Quantitative Real-Time Polymerase Chain Reaction (PCR). Total RNA was isolated from scraped epidermis using TRIzol Reagent according to the manufacturer's instruction (Invitrogen, Carlsbad, CA). A total of 2 μg of RNA was transcribed into cDNA using SuperScript II Reverse Transcriptase (Invitrogen, Renfrewshire, U.K.) in a final volume of 20 μL at 42 °C for 50 min and 99 °C for 5 min. Real-time PCR reactions were performed in LightCycler TaqMan Master kit and LightCycler 1.5 System (Roche Diagnostics, Inc., Rotkreuz, Switzerland) according to the manufacturer's instruction. Specific primers and TaqMan probes used in this experiment are designed to target the conserved regions of various genes using the LightCycler probe design software (Roche Applied Science, Indianapolis, IN) and are listed as described before.[30] The thermal cycling conditions are 5 min at 94 °C followed by 45 cycles, in which each cycle was at 94 °C for 15 s and at 60 °C for 1 min. The relative expression level of the gene in samples was calculated with the LightCycler software, normalized with housekeeping control (β-actin).

Preparation of Cytosolic and Nuclear Extracts from Epidermis. Cytosolic and nuclear protein extractions were prepared as described previously.[30] Briefly, the epidermis was homogenized in 0.2 mL of ice-cold hypotonic buffer A containing 10 mM *N*-hydroxyethylpiperazine-*N*′-2-ethanesulfonic acid (pH 7.8), 10 mM KCl, 2 mM $MgCl_2$, 1 mM DTT, 0.1 mM EDTA, and 0.1 mM PMSF with a Polytron for 1 min. The homogenates were incubated on ice with gentle shaking for 15 min and centrifuged at 1000 rpm for 5 min. The supernatant was collected as a cytosolic fraction. The pellet was washed by resuspending in buffer A supplemented with 50 μL of 10% NP-40, vortexed, and centrifuged for 2 min at 14 000 rpm. The nuclear pellet was resuspended in 200 μL of high salt extraction buffer C [50 mM *N*-hydroxyethylpiperazine-*N*′-2-ethanesulfonic acid (pH 7.8), 50 mM KCl, 300 mM NaCl, 0.1 mM EDTA, 1 mM DTT, 0.1 mM PMSF, and 10% glycerol]. It was kept on ice for 30 min followed by centrifugation at 12 000 rpm for 30 min. The supernatant was collected as a nuclear fraction. Both cytosolic and nuclear fractions were stored at −70 °C for further Western blot analysis.

Measurement of Ear Edema and Epidermal Hyperplasia. To measure ear edema, both ears of each mouse were pretreated with HBA for 30 min and then topically applied with 1 nmol of TPA. Mice were sacrificed by CO_2 asphyxiation at 8 h after TPA administration, and the ear were excised immediately. Ear punch biopsies (5 mm in diameter) were obtained for measurement of the ear thickness and weight. In the epidermal thickness study, skin samples from different treatment groups were fixed in 10% formalin and embedded in paraffin for histological examinations. Sections (4 μm in thickness) of the skin samples were cut and mounted on polylysin-coated slides. Each section was deparaffinized in xylene, rehydrated through a series of graded alcohols, and subjected to stain with hematoxylin and eosin. The thickness of the epidermis (μm) was measured using a Nikon light microscope (Japan) equipped with an ocular micrometer by the magnification (400×) in 15 fields per section. The number of dermal infiltrating inflammatory cells was determined by counting the stained cells at five different areas.

Two-Stage Mouse Skin Carcinogenesis. Female ICR mice were randomly divided into four groups of 12 animals each. These animals were given commercial rodent pellets and fresh tap water ad libitum, both of which were changed twice a week. The dorsal regions of all mice were shaved and treated with 200 nmol of DMBA in 200 μL of acetone. One week after initiation, the mice were topically treated with 200 μL of acetone or 5 nmol of TPA in 200 μL of acetone twice a week for 20 weeks. To examine antitumor promoting activity of HBA, the DMBA-initiated mice were treated with HBA (1 or 10 mg in 200 μL of acetone) before each TPA application. Tumors of at least 1 mm diameter in an electronic digital caliper were counted and recorded twice every week, and the diameters of skin tumors were measured at the same time. The results were expressed as the average number of tumors per mouse, percentage of tumor-bearing mice, and tumor size distribution per mouse.

Statistical Analyses. All data are presented as means ± standard deviation (SD) of at least three independent experiments. Comparisons were subjected to one-way analysis of Student's *t* test, and statistical significance was defined as $p < 0.05$.

RESULTS

HBA Suppressed TPA-Induced iNOS, COX-2, and ODC Expression in Mouse Skin. The effects of HBA (Figure 1) on TPA-induced expression of inflammatory iNOS and COX-2 were investigated. As illustrated in Figure 2A, topically applied TPA in mouse skin induced maximal protein expression of iNOS at 2 h. Up-regulated COX-2 protein level was observed at 2 h and increased at 4 h. TPA is known to induce ODC, a rate-limiting enzyme in the synthesis of polyamines that play a pivotal role in cell growth and proliferation.[7] TPA treatment elevated the ODC protein level at 2 h and markedly increased it at 4 h. In contrast, administration of HBA 30 min prior to TPA treatment notably reduced the protein levels of iNOS, COX-2, and ODC in a concentration-dependent manner, whereas the protein expression of constitutive COX-1 was not affected (Figure 2B). Real time PCR was done to investigate whether HBA suppressed gene expression of iNOS, COX-2, and ODC caused by TPA. As shown in Figure 2C, pretreatment with HBA significantly attenuated iNOS, COX-2, and ODC gene expressions in a dose-dependent manner that was consistent with the results from Western blot analysis.

HBA Suppressed TPA-Induced NF-κB Nuclear Translocation and IκB Degradation in Mouse Skin. Further, we examined the molecular targets attribute to HBA suppressing TPA-induced inflammatory enzymes expression in mouse skin. Transcription factor NF-κB is critical for up-regulation of both iNOS and COX-2 in response to inflammatory stimulation.[31] Therefore, we first investigated the effect of HBA on TPA-induced activation of NF-κB. Phosphorylation and proteolytic degradation of IκB, an inhibitor of NF-κB, is the most important mechanism for activation of NF-κB by releasing from the cytoplasmic NF-κB−IκB complex and further nuclear translocation. It was found that TPA application caused the serine phosphorylation of IκBα protein accompanied with its degradation (Figure 3A). Pretreatment of HBA effectively repressed the phosphorylation and degradation of IκBα caused by TPA. The translocation of NF-κB was measured by extracts of nucleus and cytosol from mouse epidermis and subjected to Western Blot analysis. As presented in Figure 3B, TPA evoked nuclear translocation of both NF-κB subunits, p50 and p65, and was strongly inhibited by HBA pretreatment. HBA inhibited nuclear translocation of p50 and p65 was followed by sustaining their cytosolic levels. The nuclear level of phosphor-p65 (Ser536), which contributes to its transcriptional activity, was also reduced by HBA administration. These results suggested that HBA suppressed inflammatory iNOS and COX-2 expression in TPA-stimulated mouse skin might be through blocking the degradation of IκBα protein and subsequently translocation of NF-κB to the nucleus.

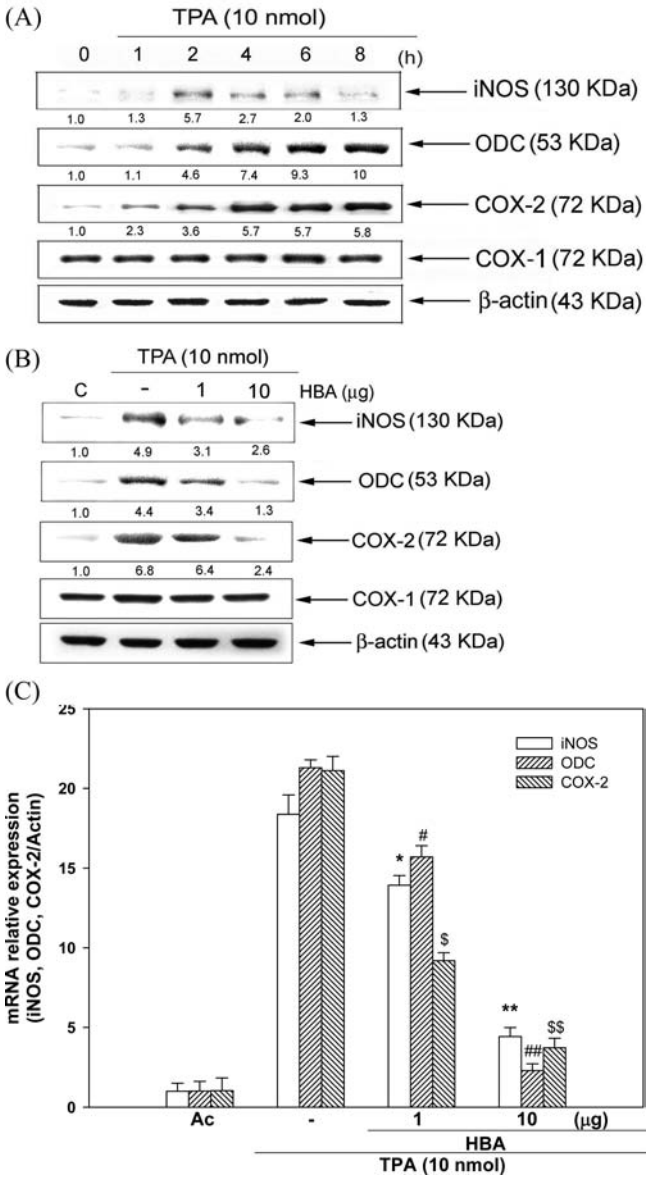

Figure 2. Effects of HBA on TPA-induced protein and gene expression of iNOS, COX-2, and ODC. Animals were treated as described in the Materials and Methods section. (A) After topical application of TPA, mice were sacrificed at the indicated time. The time courses for iNOS, COX-2, and ODC protein expression were analyzed by Western blotting. (B) Mice were pretreated with HBA at 1 and 10 μg, and the total epidermal protein was extracted and analyzed for the protein level of iNOS (2 h), COX-2 (4 h), and ODC. (C) Total RNA extracted from epidermis after TPA application at 1 h (iNOS) and 2 h (COX-2 and ODC), respectively, The gene expression of iNOS, COX-2, and ODC was performed using the LightCycler System and TaqMan probe real-time PCR. Data are presented as mean ± SE of triplicate independent experiments. $^{*}P < 0.01$, $^{**}P < 0.001$ (for iNOS), $^{\#}P < 0.01$, $^{\#\#}P < 0.001$ (for COX-2), and $^{\$}P < 0.01$, $^{\$\$}P < 0.001$ (for ODC) were compared with TPA-treated alone group. Ac, acetone.

Inhibitory Effects of HBA on Phosphorylation of MAPK Kinases and PI3K/Akt in TPA-Treated Mouse Skin. MAPKs are important intracellular signaling molecules that responded to various stimulations. MAPKs and PI3K/Akt signaling pathways have been shown to up-regulate inflammatory mediators through activation of NF-κB or AP-1 in TPA-stimulated mouse skin.[21,32,33] We investigated the effects of

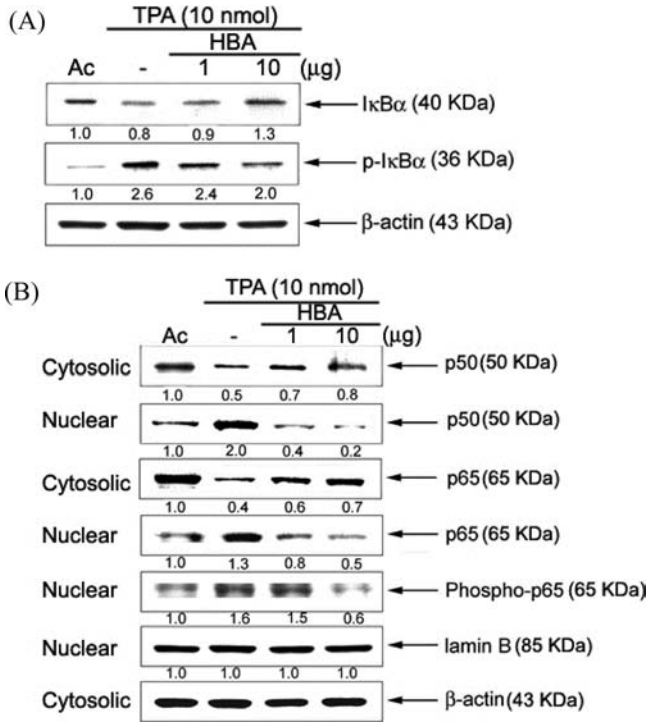

Figure 3. Inhibitory effects of HBA on TPA-induced nuclear translocation of NF-κB in mouse skin. Mice were pretreated with HBA and sacrificed at 1 h after treatment of TPA (A); the total protein was extracted from epidermis for analysis of phospho-IκBα and total IκBα. (B) Nuclear and cytosolic fractions were assayed for phospho-p65 (Ser536), p65, and p50. Lamin B and β-actin were used as internal controls for nuclear and cytosolic fraction, respectively. Data are representative of at least three independent experiments, which showed a similar result. Ac, acetone.

HBA on the phosphorylation of p38, ERK1/2, JNK1/2, PI3K, and Akt by Western blotting. As shown in Figure 4A and B, phosphorylation of p38, ERK1/2, and JNK1/2 was observed in response to TPA application compared to acetone-treated mice. Pretreatment with HBA markedly reduced phosphorylation of p38, ERK1/2, and JNK1/2 in a dose-dependent manner. TPA treatment also induced the phosphorylation of PI3K and its downstream target Akt (Figure 4C), while both were attenuated by pretreatment with HBA. The total protein levels of MAPKs and PI3K/Akt were not affected by TPA or HBA treatment. These results indicated that HBA suppressed TPA-induced NF-κB activation in mouse skin might be through interrupting MAPKs and PI3K/Akt signaling, which further block downstream iNOS and COX-2 gene expression.

Effects of HBA on TPA-Induced Ear Edema and Epidermal Hyperplasia. The anti-inflammatory activity of HBA was evaluated in a mouse ear edema model induced by TPA. Table 1 summarized ear edema induced by a single topical application of TPA at 1 nmol that presented as increased ear weight and thickness compared to acetone treatment. Topical application of HBA prior to TPA treatment resulted in significantly decreased ear weight and thickness in a concentration-dependent manner. Compared to the TPA-treated alone group, HBA pretreatment inhibited ear edema approximately by 30−50% (Table 1). TPA-induced skin inflammation was also performed to examine the effect of HBA on epidermal hyperplasia and infiltration of inflammatory cells. Histological results (Figure 5A and B) demonstrated that

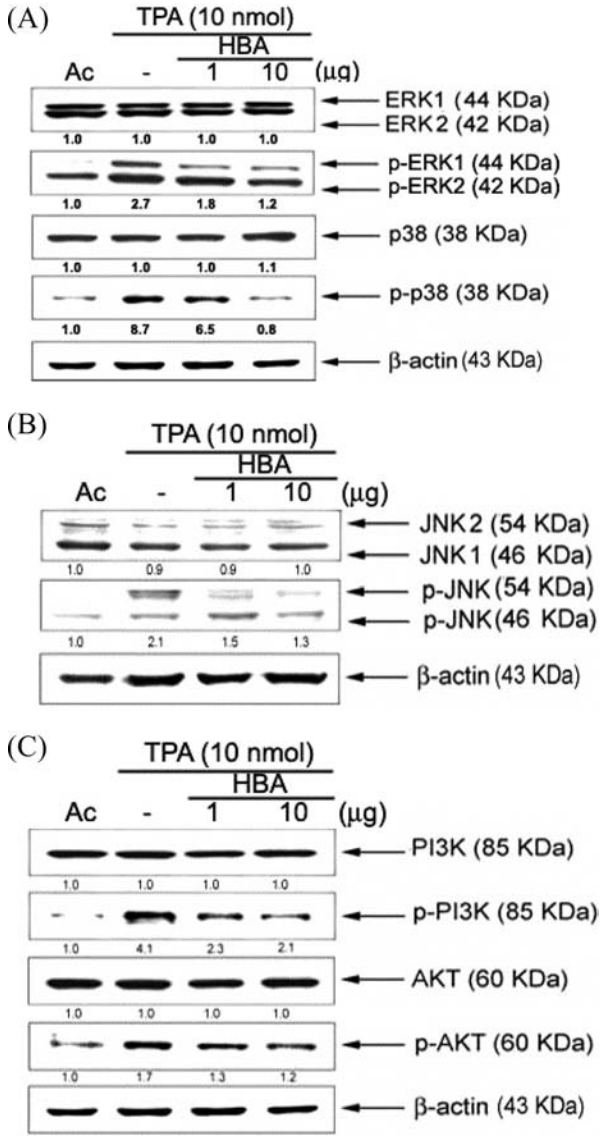

Figure 4. Effects of HBA on TPA-induced activation of MAPKs and PI3K/Akt signaling in mouse skin. Mice treatment as described in the Materials and Methods section. Protein lysates were prepared from epidermis at 1 h after treatment with TPA. Levels of (A) p-ERK1/2, total ERK, p-p38, total p38; (B) p-JNK1/2, total JNK1/2; (C) p-PI3K, total PI3K, p-Akt, and total Akt were analyzed by Western blot analysis.

TPA application in a dose of 10 nmol caused a significant increase in epidermal thickness as compared to acetone-treated mice at 34.1 ± 4.6 and 15.1 ± 0.3 μm ($P < 0.001$), respectively. Pretreatment HBA suppressed TPA caused epidermal hyperplasia in a dose-dependent manner which presented as 27.3 ± 2.1 μm ($P < 0.05$) and 22.4 ± 5.4 μm ($P < 0.01$), respectively. The marked infiltration of inflammatory cells was found in TPA-stimulated mouse skin (Figure 5A and C) at 24 h compared to acetone treatment (716.7 ± 65.1/mm^2 and 20.2 ± 2.0/mm^2, respectively) ($P < 0.001$). Topical application of HBA at 1 and 10 μg prior to TPA dramatically and significantly reduced the infiltrated inflammatory cells to 220.7 ± 54.0/mm^2 ($P < 0.01$) and 89.3 ± 32.7/mm^2 ($P < 0.001$), respectively.

HBA Suppressed DMBA/TPA-Induced Mouse Skin Carcinogenesis. The antitumor promoting activity of HBA was investigated in DMBA-initiated and TPA-induced tumor promotion in mouse skin. At the end of 20 weeks, the body weight in each group did not differ throughout the study (Figure 6A). Furthermore, the mean weights of liver and spleen were shown no significant difference among the groups (data not shown), indicating HBA treatment did not cause any noticeable side effect or toxicity. Figure 6B and C showed the average papillomas per mouse in the DMBA-initiated and TPA-treated group was 17.2 ± 0.9 with a 100% tumor incidence at the 20th week. In contrast, no papilloma was observed by acetone treatment in DMBA-initiated mice. Application of HBA at 1 and 10 μg 30 min prior to each TPA treatment for 20 weeks resulted in significant reduction in the average number of papillomas as 5.1 ± 1.2 ($P < 0.01$) and 2.3 ± 1.2 ($P < 0.001$), respectively, compared to TPA-treated mice. The tumor incidence was also lowered to 75 and 58.7% by 1 and 10 μg of HBA pretreatment, respectively ($P < 0.05$ and $P < 0.01$). The antitumor promoting effect of HBA was also analyzed in terms of the size distribution of papillomas and compared with TPA-treated mice. As presented in Table 2, the size of papilloma per mouse was dose-dependently lowered in the HBA-treated group. Pretreatment significantly decreased the number of papillomas per mouse at 3 to <5 and ≥5 mm compared with the TPA-treated mouse. Comparing the weight of papilloma in all groups, mice in the TPA-treated group showed an average tumor weight of 0.76 ± 0.04 g, whereas the average tumor weight was significantly decreased in the HBA pretreated groups to 0.34 ± 0.14 g ($P < 0.01$) and 0.09 ± 0.10 g ($P < 0.001$), respectively. HBA treatment decreased papilloma size and weight, indicating its ability in reduction of tumor growth.

DISCUSSION

Chronic inflammation is a critical component in cancer development and has been considered as a promising target in cancer chemoprevention.[3,15] Inflammation is involved in every stage of cancer development; however, interference with

Table 1. Inhibitory Effect of HBA on TPA-Induced Mouse Ear Edema[a]

	ear weight		ear thickness	
treatment	mg	inhibition (%)	mm	inhibition (%)
Ac/Ac	5.7 ± 1.6		0.12 ± 0.01	
Ac/TPA	15.1 ± 1.2[b]		0.62 ± 0.01[b]	
HBA 1 μg/TPA	10.8 ± 1.5[c]	28.5	0.41 ± 0.02[c]	32.3
HBA 10 μg/TPA	8.5 ± 1.1[d]	43.7	0.32 ± 0.03[d]	48.4

[a]Female ICR mice received vehicle (Ac) or HBA (1 or 10 μg) 30 min prior to each topical application of TPA (1 nmol). Eight hours later, the mice were killed and the ears were removed to measure the ear weight and thickness. The average number of ear weight and thickness were expressed as mean ± SE per mouse ($n = 6$). Ac, acetone. [b]$p < 0.05$, compared with the Ac/Ac group. [c]$p < 0.01$, compared with the Ac/TPA group. [d]$p < 0.001$, compared with the Ac/TPA group.

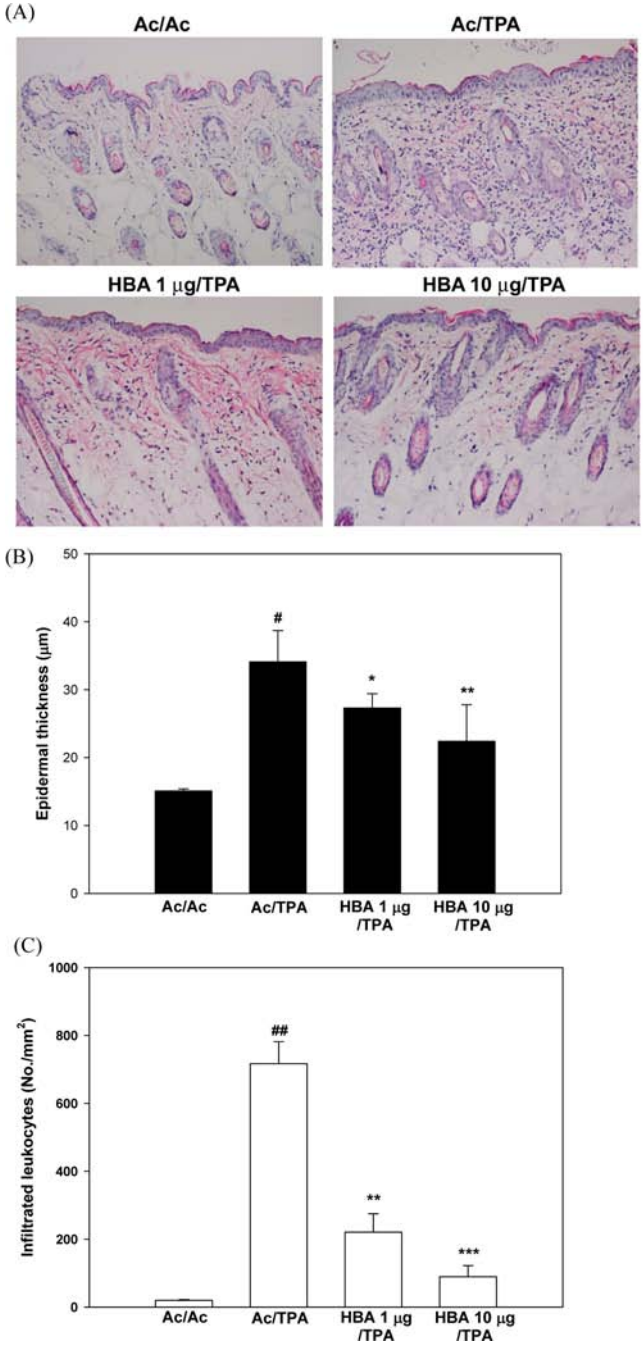

Figure 5. Inhibitory effect of HBA on TPA-induced epidermal thickness and infiltrated inflammatory cells in mouse skin. Animals were pretreated with HBA and sacrificed at 24 h after TPA treatment. The skin section were embedded in paraffin for (A) HE staining, (B) epidermal thickness (μm), and (C) infiltrated inflammatory cells (no. per mm^2) as described in the Materials and Methods section. $^{\#}P <$ 0.001 compared to Ac/Ac-treated mice. $^{*}P < 0.05$, $^{**}P < 0.01$, and $^{***}P < 0.001$ were compared with the Ac/TPA-treated group. Ac, acetone.

the promotion stage appears to be a more appropriate and efficacious approach for cancer prevention and intervention than initiation stage with irreversible gene mutation.[5] Numerous phytochemicals are demonstrated to be chemopreventive agents through their anti-inflammatory properties involving diverse mechanisms such as modulation of inflammatory signaling, reduction of inflammatory molecule production, and diminishing recruitment and activation of inflammatory cells.[2,15] In the present study, for the first time, we showed that topical application of HBA effectively suppressed TPA-mediated inflammatory responses and DMBA/TPA-induced skin carcinogenesis by targeting multiple cellular signaling and biological events.

The *in vivo* anti-inflammatory activity was first investigated by TPA-stimulated mouse skin. TPA is a potent tumor promoter which caused proliferation of epidermal cells and histological and biochemical alterations implicated in inflammatory response, leading to skin tumor promotion.[7] In our present study, we found that TPA treatment induced both protein and gene expressions of inflammatory mediators iNOS and COX-2 as well as proliferative marker, ODC. Topical application of HBA prior to TPA significantly inhibited protein and gene levels of iNOS, COX-2, and ODC caused by TPA in a concentration-dependent manner (Figure 2). Both iNOS and COX-2 are constitutively overexpressed in various human inflammatory conditions and malignancies as well as DMBA/TPA-induced skin papilloma, which are considered potential molecular targets for cancer chemoprevention.[2] Inhibition of iNOS by aminoguanidine lowered the number of papillomas in DMBA/TPA-treated mouse skin.[9] Excessive cytokine PGE2 produced by COX-2 has been shown to have implications in epidermal proliferation, vascular permeability, and skin tumorigenesis.[34] Elevated epidermal ODC by tumor promoters is attributed to cell proliferation, apoptosis reduction, angiogenesis, and tumor promotion.[35] In the present study, we found that pretreatment of HBA markedly reduced TPA-induced inflammatory responses including ear edema, epidermal hyperplasia, and infiltration of inflammatory cells (Table 1 and Figure 4), indicating this inhibitory effect of HBA may contribute to the suppression of inflammatory mediators and ODC.

NF-κB is the most fundamental transcription factor in regulation of iNOS and COX-2 expression, which plays a crucial role in inflammation and cancer development.[36,37] Topical application of TPA to mouse dorsal skin induced expression of iNOS and COX-2 through activation of NF-κB. In the current study, HBA treatment was found to attenuate TPA-induced nuclear translocation of p50 and p65 by reducing phosphorylation and degradation of IκBα protein (Figure 3). We previously reported that mouse dorsal skin treated with TPA induced an inflammatory response and expression of iNOS, COX-2, and ODC but were suppressed by preapplication of NF-κB inhibitor, PDTC. Moreover, phosphorylation of p65 at serine 536 by IKK within the transactivation domain is important for its transcriptional activation.[38] Pretreatment of HBA abolished nuclear levels of phospho-p65 (Ser536) thus may affect its transcriptional function on activation of iNOS and COX-2 (Figure 3B). Furthermore, Lee et al. have reported the humulone, α-acid in hop, directly inhibited IKKβ activity *in vitro* and in TPA-stimulated mouse skin[21] which indicated HBA might have a similar effect on IKK activity due to their similar structures. However, the detailed mechanism remains to be elucidated. These results suggested that suppression of NF-κB activation by HBA might be a major target for its anti-inflammatory efficacy.

Activation of MAPKs and PI3K/Akt signaling is involved in a variety of cellular functions and plays a pivotal role in inflammation and tumorigenesis.[39,40] Up-regulated MAPKs and PI3K/Akt signaling contribute to activation of NF-κB and AP-1, as well as downstream expression of inflammatory

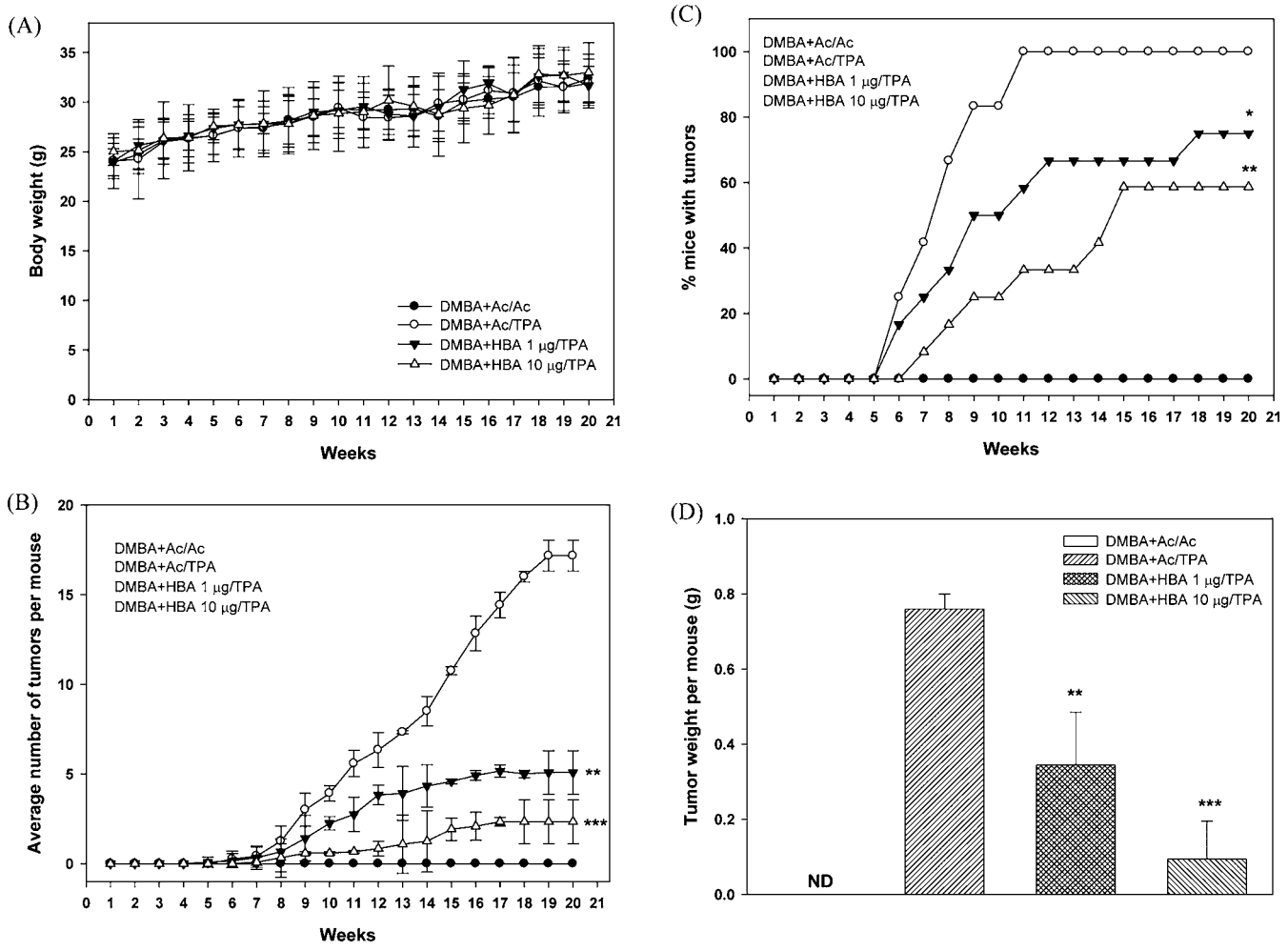

Figure 6. Antitumor-promoting effects of HBA on DMBA/TPA-induced skin tumorigenesis in ICR mice. Tumor promotion in all mice was initiated with DMBA (200 nmol) and promoted with TPA (5 nmol) twice weekly, starting 1 week after initiation. HBA (1 and 10 μg) was dissolved in 0.2 mL of acetone and topically applied 30 min prior to each TPA treatment. Tumors of at least 1 mm in diameter were counted and recorded weekly, as described in the Materials and Methods section. (A) The body weight of mice during skin tumor promotion. (B) Average number of tumors per mouse. (C) Percentage of tumor-bearing mice (tumor incidence). (D) Tumor weight per mouse. *P < 0.0, **P < 0.01, and ***P < 0.001 were compared with the Ac/TPA-treated group. Ac, acetone. ND, not detected.

Table 2. Effects of HBA on Tumor Diameter in DMBA/TPA-Induced Skin Tumorigenesis[a]

	tumor size (mm)		
treatment	1 to <3	3 to <5	≥5
DMBA + Ac/Ac			
DMBA + Ac/TPA	5.7 ± 1.4	9.7 ± 1.4	3.7 ± 1.0
DMBA + HBA 1 μg/TPA	3.5 ± 0.1	1.3 ± 1.1[c]	0.3 ± 0.7[c]
DMBA + HBA 10 μg/TPA	1.6 ± 1.4[b]	0.4 ± 0.9[d]	0.5 ± 0.5[c]

[a]The diameters of skin tumors were measured by an electronic digital caliper twice every week. The tumor size was recorded as the average of length × width (mm) per mouse (n = 12). Ac, acetone. [b]p < 0.05. [c]p < 0.01. [d]p < 0.001 were compared with the Ac/TPA group.

mediators in TPA-treated mouse skin. Administration of specific inhibitors of MAPKs is shown to attenuate TPA-stimulated COX-2 expression by blocking activation of different transcription factors.[21,32,33] Here we explored the effect of HBA on these upstream kinases and found that HBA effectively reduced TPA caused phosphorylation of ERK1/2, p38 MAPK, and JNK1/2 in mouse skin (Figure 4A and B), suggesting HBA diminished NF-κB activation possibly through targeting of these kinases. In addition, down-regulated PI3K/Akt signaling by specific inhibitor, LY294002, has been reported to inhibit NF-κB DNA binding activity and COX-2 expression in TPA-treated HR-1 hairless mouse skin.[41] In the results of this study, the inhibitory effect of HBA on activation of PI3K/Akt signaling was also observed (Figure 4C). Therefore, we suggested HBA suppressed TPA-induced NF-κB activation and downstream inflammatory mediators possibly not only through blockage of MAPK signaling but also interference with the PI3K/Akt signaling pathway, subsequently suppressing the gene transcription of iNOS and COX-2.

We performed the classical two-stage skin carcinogenesis induced by DMBA/TPA in mouse skin to further examine the antitumor promotional efficacy of HBA. Our results clearly demonstrated that administration of HBA prior to TPA treatment in the promotion stage significantly and effectively lowered the number and incidence of papillomas in a dose-dependent manner (Figure 6B and C). By measurement of the diameter and weight of skin papilloma, we also found that the size and weight of papillomas were decreased by HBA pretreatment (Figure 6D and E). Previously, Yasukawa et al. have reported that application of humulone at 1 mg reduced

dx.doi.org/10.1021/jf403560r | J. Agric. Food Chem. 2013, 61, 11541−11549

skin tumor formation in a two-stage carcinogenesis model.[42] Here we found that treatment of HBA at 1 and 10 μg displayed a potent inhibitory effect on reduction of skin papilloma. The probable mechanism of HBA to reduce skin papilloma formation may result from its anti-inflammatory property through suppression of inflammatory mediators, epidermal hyperplasia, and inflammatory cells infiltrating. Therefore, HBA may have great potential as a novel chemopreventive agent to be used in the treatment of inflammation associated with tumorigenesis.

AUTHOR INFORMATION

Corresponding Author

*Address: Institute of Food Science and Technology, National Taiwan University No.1, Section 4, Roosevelt Road, Taipei 10617, Taiwan. Phone: (886)-2-33664133 E-mail: mhpan@ntu.edu.tw.

Author Contributions

○These authors contributed equally to this work.

Funding

This study was supported by the National Science Council NSC 101-2628-B-022-001-MY4, 102-2628-B-002-053-MY3 and Taipei Medical University Hospital, 99TMU-TMUH-01-04.

Notes

The authors declare no competing financial interest.

ABBREVIATIONS USED

iNOS, inducible nitric oxide synthase; LPS, lipopolysaccharide; NO, nitric oxide; COX-2, cycoloxygenase-2; PGE_2, prostaglandin E_2; IκB, inhibitor κB; NF-κB, nuclear factor-κB; MAPK, mitogen-activated protein kinase; C/EBP, CCAAT/enhancer-binding protein; STAT3, signal transducer and activator of transcription 3

REFERENCES

(1) Libby, P. Inflammatory mechanisms: the molecular basis of inflammation and disease. *Nutr. Rev.* **2007**, *65*, S140−S146.

(2) Pan, M. H.; Lai, C. S.; Dushenkov, S.; Ho, C. T. Modulation of inflammatory genes by natural dietary bioactive compounds. *J. Agric. Food Chem.* **2009**, *57*, 4467−4477.

(3) Colotta, F.; Allavena, P.; Sica, A.; Garlanda, C.; Mantovani, A. Cancer-related inflammation, the seventh hallmark of cancer: links to genetic instability. *Carcinogenesis* **2009**, *30*, 1073−1081.

(4) Mantovani, A. Molecular pathways linking inflammation and cancer. *Curr. Mol. Med.* **2010**, *10*, 369−373.

(5) Wu, X.; Pandolfi, P. P. Mouse models for multistep tumorigenesis. *Trends Cell Biol.* **2001**, *11*, S2−S9.

(6) Dipple, A.; Pigott, M. A.; Bigger, C. A.; Blake, D. M. 7,12-dimethylbenz[a] anthracene - DNA binding in mouse skin: response of different mouse strains and effects of various modifiers of carcinogenesis. *Carcinogenesis* **1984**, *5*, 1087−1090.

(7) Raick, A. N. Ultrastructural, histological, and biochemical alterations produced by 12-O-tetradecanoyl-phorbol-13-acetate on mouse epidermis and their relevance to skin tumor promotion. *Cancer Res.* **1973**, *33*, 269−286.

(8) Murakawa, M.; Yamaoka, K.; Tanaka, Y.; Fukuda, Y. Involvement of tumor necrosis factor (TNF)-alpha in phorbol ester 12-O-tetradecanoylphorbol-13-acetate (TPA)-induced skin edema in mice. *Biochem. Pharmacol.* **2006**, *71*, 1331−1336.

(9) Chun, K. S.; Cha, H. H.; Shin, J. W.; Na, H. K.; Park, K. K.; Chung, W. Y.; Surh, Y. J. Nitric oxide induces expression of cyclooxygenase-2 in mouse skin through activation of NF-kappaB. *Carcinogenesis* **2004**, *25*, 445−454.

(10) Lai, C. S.; Li, S.; Chai, C. Y.; Lo, C. Y.; Dushenkov, S.; Ho, C. T.; Pan, M. H.; Wang, Y. J. Anti-inflammatory and antitumor promotional effects of a novel urinary metabolite, 3′,4′-didemethylnobiletin, derived from nobiletin. *Carcinogenesis* **2008**, *29*, 2415−2424.

(11) Chun, K. S.; Kim, S. H.; Song, Y. S.; Surh, Y. J. Celecoxib inhibits phorbol ester-induced expression of COX-2 and activation of AP-1 and p38 MAP kinase in mouse skin. *Carcinogenesis* **2004**, *25*, 713−722.

(12) Guha, M.; Mackman, N. LPS induction of gene expression in human monocytes. *Cell Signalling* **2001**, *13*, 85−94.

(13) Kuo, D. H.; Lai, Y. S.; Lo, C. Y.; Cheng, A. C.; Wu, H.; Pan, M. H. Inhibitory effect of magnolol on TPA-induced skin inflammation and tumor promotion in mice. *J. Agric. Food Chem.* **2010**, *58*, 5777−5783.

(14) Yoon, J. H.; Lim, T. G.; Lee, K. M.; Jeon, A. J.; Kim, S. Y.; Lee, K. W. Tangeretin reduces ultraviolet B (UVB)-induced cyclooxygenase-2 expression in mouse epidermal cells by blocking mitogen-activated protein kinase (MAPK) activation and reactive oxygen species (ROS) generation. *J. Agric. Food Chem.* **2011**, *59*, 222−228.

(15) Pan, M. H.; Lai, C. S.; Ho, C. T. Anti-inflammatory activity of natural dietary flavonoids. *Food Funct.* **2010**, *1*, 15−31.

(16) Van, Cleemput, M.; Cattoor, K.; De, Bosscher, K.; Haegeman, G.; De, Keukeleire, D.; Heyerick, A. Hop (*Humulus lupulus*)-derived bitter acids as multipotent bioactive compounds. *J. Nat. Prod.* **2009**, *72*, 1220−1230.

(17) Tagashira, M.; Watanabe, M.; Uemitsu, N. Antioxidative activity of hop bitter acids and their analogues. *Biosci. Biotechnol. Biochem.* **1995**, *59*, 740−742.

(18) Siragusa, G. R.; Haas, G. J.; Matthews, P. D.; Smith, R. J.; Buhr, R. J.; Dale, N. M.; Wise, M. G. Antimicrobial activity of lupulone against Clostridium perfringens in the chicken intestinal tract jejunum and caecum. *J. Antimicrob. Chemother.* **2008**, *61*, 853−858.

(19) Van Cleemput, M.; Heyerick, A.; Libert, C.; Swerts, K.; Philippe, J.; De Keukeleire, D.; Haegeman, G.; De Bosscher, K. Hop bitter acids efficiently block inflammation independent of GRalpha, PPARalpha, or PPARgamma. *Mol. Nutr. Food Res.* **2009**, *53*, 1143−1155.

(20) Saugspier, M.; Dorn, C.; Thasler, W. E.; Gehrig, M.; Heilmann, J.; Hellerbrand, C. Hop bitter acids exhibit anti-fibrogenic effects on hepatic stellate cells in vitro. *Exp. Mol. Pathol.* **2012**, *92*, 222−228.

(21) Lee, J. C.; Kundu, J. K.; Hwang, D. M.; Na, H. K.; Surh, Y J. Humulone inhibits phorbol ester-induced COX-2 expression in mouse skin by blocking activation of NF-kappaB and AP-1: IkappaB kinase and c-Jun-N-terminal kinase as respective potential upstream targets. *Carcinogenesis* **2007**, *28*, 1491−1498.

(22) Siegel, L.; Miternique-Gross, A.; Griffon, C.; Klein-Soyer, C.; Lobstein, A.; Raul, F.; Stephan, D. Antiangiogenic properties of lupulone, a bitter acid of hop cones. *Anticancer Res.* **2008**, *28*, 289−294.

(23) Lamy, V.; Roussi, S.; Chaabi, M.; Gosse, F.; Lobstein, A.; Raul, F. Lupulone, a hop bitter acid, activates different death pathways involving apoptotic TRAIL-receptors, in human colon tumor cells and in their derived metastatic cells. *Apoptosis* **2008**, *13*, 1232−1242.

(24) Lamy, V.; Roussi, S.; Chaabi, M.; Gosse, F.; Schall, N.; Lobstein, A.; Raul, F. Chemopreventive effects of lupulone, a hop {beta}-acid, on human colon cancer-derived metastatic SW620 cells and in a rat model of colon carcinogenesis. *Carcinogenesis* **2007**, *28*, 1575−1581.

(25) Stephan, T. E.; Ngo, E. O.; Nutter, L. M. Hexahydrocolupulone and its antitumor cell proliferation activity *in vitro*. *Biochem. Pharmacol.* **1998**, *55*, 505−514.

(26) Liu, Y.; Tang, J.; Liu, K.; Chen, D. Synthesis technology of hexahydro-beta-acids, a novel antibacterial agent. *Shipin Gongye Keji* **2008**, *29*, 225−229.

(27) Carson, J. F. The hydrogenation of lupulone and humulone. *J. Am. Chem. Soc.* **1951**, *73*, 1850−1851.

(28) Liu, C. B.; Chen, L. H.; Cheng, A. C.; Chen, W. J.; Tsai, M. L.; Liu, Y.; Ho, C. T.; Pan, M. H. Hexahydro-beta-acids induce apoptosis through mitochondrial pathway, GADD153 expression, and caspase

activation in human leukemia cells. *Food Chem. Toxicol.* **2011**, *49*, 1033−1042.
(29) Tang, W.; Chen, L. H.; Daun, H.; Ho, C. T.; Pan, M. H. Inhibitory effects of hexahydro-b-acids in LPS-stimulated murine macrophage. *J. Funct. Foods* **2011**, *3*, 215−222.
(30) Lai, C. S.; Li, S.; Chai, C. Y.; Lo, C. Y.; Ho, C. T.; Wang, Y. J.; Pan, M. H. Inhibitory effect of citrus 5-hydroxy-3,6,7,8,3′,4′-hexamethoxyflavone on 12-O-tetradecanoylphorbol 13-acetate-induced skin inflammation and tumor promotion in mice. *Carcinogenesis* **2007**, *28*, 2581−2588.
(31) Tak, P. P.; Firestein, G. S. NF-kappaB: a key role in inflammatory diseases. *J Clin. Invest.* **2001**, *107*, 7−11.
(32) Kim, S. O.; Kundu, J. K.; Shin, Y. K.; Park, J. H.; Cho, M. H.; Kim, T. Y.; Surh, Y. J. [6]-Gingerol inhibits COX-2 expression by blocking the activation of p38 MAP kinase and NF-kappaB in phorbol ester-stimulated mouse skin. *Oncogene* **2005**, *24*, 2558−2567.
(33) Chun, K. S.; Keum, Y. S.; Han, S. S.; Song, Y. S.; Kim, S. H.; Surh, Y. J. Curcumin inhibits phorbol ester-induced expression of cyclooxygenase-2 in mouse skin through suppression of extracellular signal-regulated kinase activity and NF-kappaB activation. *Carcinogenesis* **2003**, *24*, 1515−1524.
(34) Rundhaug, J. E.; Pavone, A.; Kim, E.; Fischer, S. M. The effect of cyclooxygenase-2 overexpression on skin carcinogenesis is context dependent. *Mol. Carcinog.* **2007**, *46*, 981−992.
(35) O'Brien, T. G.; Megosh, L. C.; Gilliard, G.; Soler, A. P. Ornithine decarboxylase overexpression is a sufficient condition for tumor promotion in mouse skin. *Cancer Res.* **1997**, *57*, 2630−2637.
(36) Kujubu, D. A.; Fletcher, B. S.; Varnum, B. C.; Lim, R. W.; Herschman, H. R. TIS10, a phorbol ester tumor promoter-inducible mRNA from Swiss 3T3 cells, encodes a novel prostaglandin synthase/cyclooxygenase homologue. *J. Biol. Chem.* **1991**, *266*, 12866−12872.
(37) Lowenstein, C. J.; Alley, E. W.; Raval, P.; Snowman, A. M.; Snyder, S. H.; Russell, S. W.; Murphy, W. J. Macrophage nitric oxide synthase gene: Two upstream regions mediate induction by interferon r and lipopolysaccharide. *Proc. Natl. Acad. Sci. U.S.A.* **1993**, *90*, 9734.
(38) Sakurai, H.; Chiba, H.; Miyoshi, H.; Sugita, T.; Toriumi, W. IkappaB kinases phosphorylate NF-kappaB p65 subunit on serine 536 in the transactivation domain. *J. Biol. Chem.* **1999**, *274*, 30353−30356.
(39) Huang, P.; Han, J.; Hui, L. MAPK signaling in inflammation-associated cancer development. *Protein Cell* **2010**, *1*, 218−226.
(40) Luo, J.; Manning, B. D.; Cantley, L. C. Targeting the PI3K-Akt pathway in human cancer: rationale and promise. *Cancer Cell* **2003**, *4*, 257−262.
(41) Hwang, D. M.; Kundu, J. K.; Shin, J. W.; Lee, J. C.; Lee, H. J.; Surh, Y. J. cis-9,trans-11-conjugated linoleic acid down-regulates phorbol ester-induced NF-kappaB activation and subsequent COX-2 expression in hairless mouse skin by targeting IkappaB kinase and PI3K-Akt. *Carcinogenesis* **2007**, *28*, 363−371.
(42) Yasukawa, K.; Takeuchi, M.; Takido, M. Humulon, a bitter in the hop, inhibits tumor promotion by 12-O-tetradecanoylphorbol-13-acetate in two-stage carcinogenesis in mouse skin. *Oncology* **1995**, *52*, 156−158.

■ NOTE ADDED AFTER ASAP PUBLICATION

There was an error in Figure 1 in the version published November 15, 2013. The corrected version published November 27, 2013.